AIAA 81-0347R

Non-isoenergetic Turbulent Jet Mixing in a Constant-Area Duct

W. Tabakoff* and J. H. Blasenak†
University of Cincinnati, Cincinnati, Ohio

A study of non-isoenergetic turbulent jet mixing between two streams has been conducted. Using a theoretical analysis for ducted mixing, an experimental investigation was performed to verify this theory and to determine the non-isoenergetic turbulent jet mixing characteristics in a constant area duct. The described work deals with the temperature characteristics of non-isoenergetic jet mixing. Temperature profiles were measured at several axial locations in the duct for both concentric and eccentric configurations. It was determined that the theoretical and experimental temperature profiles agreed fairly well for both cases, although the concentric case showed better agreement than the eccentric case. It was concluded that the mixing theory introduced was good for a fairly simplified analysis.

Nomenclature

A = cross-sectional area of the duct, m^2 (ft^2)
AR = area ratio
C = experimental constant of turbulence (main region)
C_H = experimental constant of turbulence (initial region)
c_p = specific heat at constant pressure, cal/kg·K (Btu/lb·°R)
D = diameter of the duct, m (ft)
e = eccentricity
$\bar{e}$ = (e/R)
L = length of the duct, m (ft)
l = nondimensional length of the duct (L/D)
M = Mach number
m = (U_h/U_1)
$\dot{m}$ = mass flow rate, kg/s (lb/s)
n = bypass ratio $(\dot{m}_2/\dot{m}_1)$
p = pressure
R = radius of the duct, m (ft)
r = radial coordinate
r = radius of the free jet
r_1 = radius of the primary ejectory nozzle, m (ft)
$\bar{r}$ = (y/R)
T = temperature, K (°R)
T_t = total temperature, K (°R)
ΔT = $(T-T_2)$
U = axial velocity component, m/s (ft/s)
ΔU = $(U-U_h)$
X_k = $\sqrt{\xi_k}$
x = axial coordinate
y = transverse coordinate
α = area ratio (A_1/A_2)
β = $(\phi/\phi-1)^{1/3}$
ϕ = (T_m/T_2)
θ = temperature ratio (T_2/T_1)
ρ = density, kg/m^3 (lb/ft^3)
ξ = (y/r)
ξ_k = (R/r)
π = 3.14159...
γ = ratio of specific heats

Subscripts

1 = primary stream
2 = secondary stream
3 = completely uniform mixed flow
h = nominal wake conditions
m = at the axis
s = static
w = wall of the duct

Introduction

It is well known that at medium- and low-flight Mach numbers an exhaust gas jet of relatively small mass and high velocity is an inefficient method of producing thrust. This is due to the high energy losses at the nozzle exit and the poor use of the kinetic energy of the exhaust jet for the thrust generation. Two other important considerations for current engines are good fuel economy and a low noise level. In order to accomplish these objectives of maximizing thrust, lowering fuel consumption, and decreasing noise, a mixed-flow turbofan engine is the optimal candidate.

A high airflow is necessary to increase thrust while a high jet velocity will increase thrust but decrease propulsive efficiency. The turbofan engine produces a compromise between maximum airflow and maximum jet exhaust velocity. Theoretical studies have shown that the thrust of a turbofan engine can be increased by mixing the hot primary jet with the colder secondary airflow. Hartmann[1] confirmed these theories with his experimental investigations at a bypass ratio of 3.2. He reported a thrust gain, with equal total pressure in the primary and secondary streams before mixing, for mixing chamber inlet Mach numbers of 0.37 and below. The amount of thrust gain was a function of the stream temperature and the degree of mixing.

Therefore, it is important to optimize the amount of mixing in a turbofan nozzle. For this purpose, it is necessary to understand the mechanics of turbulent jet mixing. Although an actual turbofan engine may have turbine exit swirl and an augmentor flame holder in the flow path, a simplified analysis, which is both reliable and accurate, is necessary before the more complex problem can be solved. To satisfy this need for a tenable turbulent mixing theory, several people have made analytical studies of mixing in recent years. Several of these studies will be discussed in this paper. The theory proposed by Khanna and Tabakoff,[2] however, seemed to provide a fairly simple yet promising approach to the turbulent mixing problem. The theory lacked an experimental

Presented as Paper 81-0347 at the AIAA 19th Aerospace Sciences Meeting, St. Louis, Mo., Jan. 12-15, 1981; submitted March 9, 1981; revision received Sept. 29, 1981.

*Professor, Department of Aerospace Engineering and Applied Mechanics. Fellow AIAA.

†Graduate Research Assistant, Department of Aerospace Engineering and Applied Mechanics.

investigation of the predicted results. Therefore, the current study was performed to experimentally verify the accuracy of the theoretical analysis of turbulent jet mixing between two concentric airstreams in a constant area duct. In particular, the non-isoenergetic (different stream temperatures) case was examined. An eccentric mixing configuration was used as an additional experimental study. These two nonisoenergetic mixing studies were believed to have resulted in a better understanding of turbulent mixing in a turbofan engine.

Literature Review of Related Theories and Experiments

Free turbulent mixing has been analyzed by many authors, such as Refs. 3-9. Ducted isoenergetic turbulent mixing is examined in several works.[10-16] The best to date appears to be that of Razinsky.[17] The objective of his investigation was to determine the velocity field, the shear stress, and the pressure distribution from the well-defined step change in the velocity profile at the mixing tube entrance to the limiting condition of fully developed flow.

An experimental investigation of the isoenergetic case was conducted in Ref. 18. This study agreed with the theory of Ref. 2 for the case where the primary stream velocity was greater than the secondary stream velocity. In order to provide an additional understanding of turbulent mixing, an experimental investigation of eccentric isoenergetic ducted mixing was conducted in Ref. 19 and was compared with a slightly modified version of the theory of Ref. 2. This work was expanded by the non-isoenergetic mixing experiments discussed in this paper. Additional information on free turbulent mixing is reported in Refs. 20-23. From the literature survey, it becomes apparent that there is a lack of information concerning turbulent ducted mixing for the non-isoenergetic case.

Theoretical Analysis

A review of the theoretical analysis described by Khanna and Tabakoff[2] is appropriate since it provided the basis upon which this study expanded. They found that for free turbulent jets the differential equations were favorable to an analytical solution and the experimental behavior was quite well known. However, much less known was the behavior of a jet immersed in a secondary stream with confining walls present. Little experimental information on turbulent shear stress was available for jet flows other than free jets. Extensive measurements on free jets had shown that this type of flow was closely self-preserving up to a certain distance downstream of the nozzle exit. Reference 2 presents an analysis for turbulent jet mixing between two subsonic streams in an axisymmetric constant area duct. This analysis included both the constant temperature (isoenergetic) mixing case and the different temperatures for each stream (non-isoenergetic) mixing case.

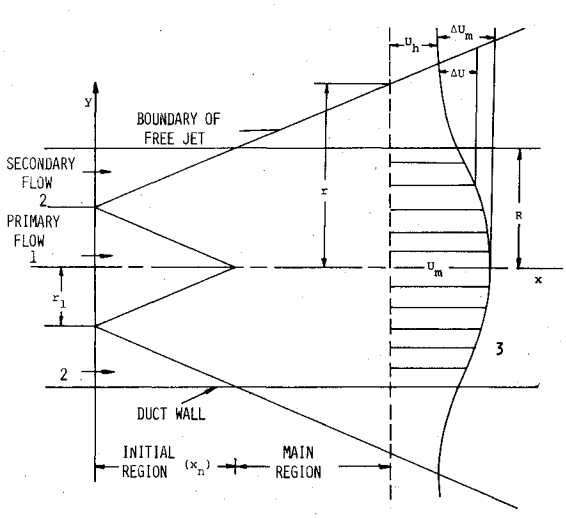

Fig. 1 Schematic diagram of confined jet mixing.

Figure 1 illustrates the schematics of the ducted mixing system. It is divided into two flow regimes which are defined as follows:

1) The initial region is where turbulent mixing occurs between the secondary flow and the core of inviscid primary flow. When the inner boundary of this mixing region intersects with the axis of the jet, the region is ended.

2) The main region is where the mixing layer has spread to the wall and no portion of undisturbed secondary flow exists. Between the initial and main regimes, the transitional region exists.

The theory used here applies only to the main region. Other assumptions used by this theory are: viscous effects at the wall are negligible, the static pressure at any cross section is constant, mixing obeys the perfect gas laws, and the duct walls are adiabatic.

Governing Equations

1) Conservation of mass. For one-dimensional steady flow the continuity equation can be written as

$$\rho_1 A_1 U_1 + \rho_2 A_2 U_2 = \rho_3 A_3 U_3 \tag{1}$$

2) Conservation of momentum. Neglecting the viscous forces acting on the walls of the mixing chamber, one can write the momentum balance equation as

$$(p_3 - p_1) A_3 = \rho_1 U_1^2 A_1 + \rho_2 U_2^2 A_2 - \rho_3 U_3^2 A_3 \tag{2}$$

3) Conservation of energy. Assuming the specific heat at constant pressure to be constant and independent of the temperature, the equation of conservation of energy is

$$\dot{m}_1 c_p T_{t_1} + \dot{m}_2 c_p T_{t_2} = \dot{m}_3 c_p T_{t_3} \tag{3}$$

4) Equation of state. For a perfect gas, this equation can be written as

$$p = \rho R T \tag{4}$$

Equations (1-4) determine the flow parameters after complete mixing, which occurs at an infinite distance from the initial cross section of the mixing chamber.

In order to determine the variation of stream velocity and temperature along the radius of the mixing chamber at any cross section, the hypothesis of universal ejection characteristics developed by Abramovich[3] will be used. This hypothesis states that the nondimensional velocity and temperature profiles at any cross section of a turbulent jet are universal functions of a parameter $\xi = (y/r)$, regardless of the external conditions of its development. By the parameter ξ definition, y is the distance from the axis in the transverse direction and r the radius of the free jet as shown in Fig. 1. This hypothesis allows the use of the results of free-jet mixing theories to determine the velocity and temperature profiles for turbulent mixing of two streams in a duct. Mathematically, one can write the universal functions for nondimensional excess velocity and the excess temperature profiles as follows:

$$\Delta U / \Delta U_m = (1 - \xi^{1.5})^2 \tag{5}$$

$$\Delta T / \Delta T_m = (1 - \xi^{1.5}) \tag{6}$$

where $\xi = (y/r)$. In a constant area mixing chamber, the maximum value of y is equal to R, the radius of the mixing chamber. The corresponding value of ξ is denoted by $\xi_k = (R/r)$, which is always less than one in the main region of the mixing chamber. Figure 1 defines the terms used in these equations. In addition, this figure illustrates the basic

concept used to find the velocity and temperature profile inside the duct. The excess velocity at the axis ΔU_m, the excess velocity ΔU, and the excess temperature ΔT are defined as follows:

$$\Delta U_m = U_m - U_h, \quad \Delta U = U - U_h, \quad \Delta T = T - T_2 \tag{7}$$

where U_m = axial velocity at the axis, U_h = nominal wake velocity, and U = axial velocity at any value of y.

The nominal wake velocity U_h can be obtained from the Bernoulli equation, if it is assumed that the main change in the pressure occurs in the initial region and that the longitudinal pressure gradient in the main region is small, i.e., a constant pressure is assumed for the whole main region. Therefore,

$$U_h^2 = U_2^2 - (2/\rho)(p_3 - p_2) \tag{8}$$

where p_3 is the pressure after completely uniform mixed flow has been attained.

One can define a criterion for the degree of mixing as the ratio of the total energy actually absorbed by the lower energy stream to the maximum absorbable total energy. The latter corresponds to perfect mixing of the streams with complete equalization of states of the mixing gases. Essentially it represents a measure of the degree of uniformity of the temperature profile in the mixing duct. The variation of the temperature along the radius of the mixing duct at any cross section will be determined by the universal function of the parameter (ξ). To determine the variation of temperature along the length of the duct, the integral relation which expresses the law of conservation of mass is written as

$$\int_0^{A_3} \rho U \mathrm{d}A = \rho_3 U_3 A_3 \tag{9}$$

Adding and subtracting the quantity

$$\int_0^{A_3} \rho U_h \mathrm{d}A$$

from Eq. (9),

$$\int_0^{A_3} \rho (U - U_h)\,\mathrm{d}A + \int_0^{A_3} \rho U_h \mathrm{d}A = \rho_3 A_3 U_3 \tag{10}$$

Since

$$A_3 = \pi R^2$$

and

$$\mathrm{d}A = 2\pi y \mathrm{d}y$$

Equation (10) becomes

$$2\int_0^R \rho \Delta U y \mathrm{d}y + 2U_h \int_0^R \rho y \mathrm{d}y = \rho_3 U_3 R^2 \tag{11}$$

For approximately constant pressure mixing, using the equation of state, the density is

$$\rho = p/RT \tag{12}$$

Substituting Eq. (4) into Eq. (11),

$$2\int_0^R (\Delta U/T) y \mathrm{d}y + 2Uh \int_0^R (y/T)\,\mathrm{d}y = U_3 R^2/T_3$$

or

$$2\int_0^{\xi_k} \frac{\Delta U_m}{T} \frac{\Delta U}{\Delta U_m} r^2 \frac{y}{r} \mathrm{d}\left(\frac{y}{r}\right) + 2U_h \int_0^{\xi_k} \frac{y}{r} \mathrm{d}\left(\frac{y}{r}\right) \Big/ T = \frac{U_3 R^2}{T_3} \tag{13}$$

or

$$2\Delta U_m \int_0^{\xi_k} \left(\frac{\Delta U/\Delta U_m}{T/T_m}\right) \xi \mathrm{d}\xi + 2U_h \int_0^{\xi_k} \frac{\xi \mathrm{d}\xi}{(T/T_m)} = U_3 \xi_k^2 (T_m/T_3) \tag{14}$$

Defining the following nondimensional parameters

$$(\rho_1/\rho_2) = \theta = (T_2/T_1),$$

$$n = (\dot{m}_2/\dot{m}_1), \quad \text{and} \quad \phi = (T_m/T_2)$$

and using the energy equation (3) it is obtained

$$\frac{T_3}{T_1} = \frac{n\theta + 1}{n + 1}$$

Now one may write

$$\frac{T_m}{T_3} = \frac{T_m}{T_2} \frac{T_2}{T_1} \frac{T_1}{T_3} = \phi\theta \left(\frac{n+1}{n\theta+1}\right) \tag{15}$$

Using Eq. (6) and the expression for ϕ, the following relation is obtained

$$\frac{T}{T_m} = \left[1 - \left(\frac{\phi - 1}{\phi}\right) \xi^{1.5}\right] \tag{16}$$

Substituting Eqs. (16), (15), and (5) into Eq. (14) results in the following:

$$\frac{\Delta U_m}{U_3} \int_0^{\xi_k} \frac{(1 - \xi^{1.5})^2 \xi \mathrm{d}\xi}{(\phi/\phi - 1) - \xi^{1.5}} + \frac{U_h}{U_3} \int_0^{\xi_k} \frac{\xi \mathrm{d}\xi}{(\phi/\phi - 1) - \xi^{1.5}} = \frac{1}{2} \xi_k^2 \left(\frac{n+1}{n\theta+1}\right) \theta(\theta - 1) \tag{17}$$

By integration of this equation, the following result is obtained

$$\frac{4}{A_1(\xi_k)} \left[\frac{\alpha(1+n\theta) - m(\alpha+1)}{\alpha\theta(n+1)}\right] \left\{\frac{X_k^7}{7} + \frac{\beta^3 - 2}{4} X_k^4 - (\beta^2 - 1)^2 \left[X_k + \frac{\beta}{6} Z_1 \frac{\beta\sqrt{3}\pi}{18}\right]\right\} + \frac{4m(\alpha+1)}{\alpha\theta(n+1)} \times \left[X_k + \frac{\beta}{6} Z_1 + \frac{\beta\sqrt{3}\pi}{18}\right] = \frac{X_k^4}{1 - \beta^3} \tag{18}$$

where:

$$X_k = \sqrt{\xi_k} \qquad \beta = (\phi/\phi - 1)^{1/3}$$

$$Z_1 = \ell n \frac{(X_k - \beta)^2}{(X_k^2 + \beta X_k + \beta^2)} - 2\sqrt{3} \tan^{-1}\left(\frac{2X_k + \beta}{\beta\sqrt{3}}\right)$$

$$A_1(\xi_k) = 1.0 - 1.143\xi_k^{1.5} + 0.4\xi_k^3$$

$$\alpha = (A_1/A_2), \quad m = (U_h/U_1) \tag{19}$$

Equation (18) implicitly determines the quantity (T_m/T_2), where T_m is the temperature on the axis of the mixing duct at any cross section. As can be seen from this equation, the quantity ϕ appears on both sides of the equation and therefore it is not possible to determine the temperature on the axis of the mixing duct for any specified location on the cross section. Instead, a trial-and-error scheme is required to determine the temperature distribution along the length of the mixing duct.

The solution of Eq. (18) was obtained through the employment of an iterative computer scheme.

Test Configuration and Description

Air is supplied from an air pressure tank at 13.608 kg/cm^2 (200 psia). The air passes through a pressure regulator in order to reduce the pressure of the flow to the desired value. The total airflow is measured with an orifice meter. The main flow is then divided into two flows, primary and secondary. The amount of mass flow in each is controlled with valves. The primary flow is routed through a pipe to the combustion chamber, which was used to heat the primary airflow. With the use of several different fuel flow nozzles and a fuel flow control panel, it was possible to regulate the primary flow temperature. The heated flow then passed through an insulated pipe until it arrived at the entrance to the mixing tunnel. The secondary air is measured with a second orifice meter and then enters a settling chamber in order to change its direction.

The primary flow passes through the settling chamber inside a 50.8 mm (2 in.) diameter pipe which can easily be exchanged with another of diameter 35.56 mm (1.4 in.). The primary flow pipe has a sharp edge so that the thickness at the initial mixing cross section is practically zero. The secondary flow is then allowed to flow coaxially with the primary flow inside the mixing duct which extends 1.52 m (5 ft) downstream. A movable rake was provided in the mixing duct. The mixing duct inside diameter was 91.6 mm (4 in.).

The flow control panel is connected to pressure lines upstream of two orifice meters and is used to assure that the air pressure after the regulator is kept constant. A switch is connected to the flow control panel which could open the air line instantaneously.

The air used during the test was supplied from a storage tank. During each run, it required 10-20 min to regulate and stabilize the desired temperature of the primary flow. Monitoring of this temperature was also required during the run in order to maintain a constant temperature. Thus, it was essential to have a system of pressure and temperature probes that could quickly measure the radial distribution at each cross section. Therefore, a temperature/pressure rake was built for the measurements.

Seven stainless steel tubes, each with an outside diameter of 3.302 mm (0.13 in.), were connected to the rake. Five of the tubes were closed at the end with a copper-constant in thermocouple. The other two tubes were used to measure the total pressure. The tubes were equally spaced from each other at multiples of 12.7 mm (0.5 in.) from the duct centerline. Each pipe was secured at its proper distance inside the wedge-shaped rake. A rake shaft was installed to insure that it moved exactly along the mixing duct axis. The rake was connected to a shaft inside of which passed the pressure probes and thermocouple wires. They ran from the rake to the appropriate data recorder instruments. The pressure probes were connected to a multitube manometer which also recorded the static pressure. The thermocouple wires were attached to a temperature recorder. The temperatures were plotted on grid paper in a different color and number for each thermocouple. The entire rake system slid along an outside scale so that an accurate position of the rake inside the mixing duct was known.

This test apparatus and instrumentations were identical to the concentric case with the exception of the position of the primary flow tube. Both the 50.8 and 35.56 mm (2.0 and 1.4 in.) diameter primary flow tubes were positioned inside of the 101.6 mm (4.0 in.) diameter duct in such a manner that their centerlines were displaced 12.7 mm (0.5 in.) below the duct centerline. Figure 2 illustrates the eccentric configuration.

Testing Procedure and Accuracy

During each run the rake was set at a certain position and the multitube manometer was read. The temperature recorder

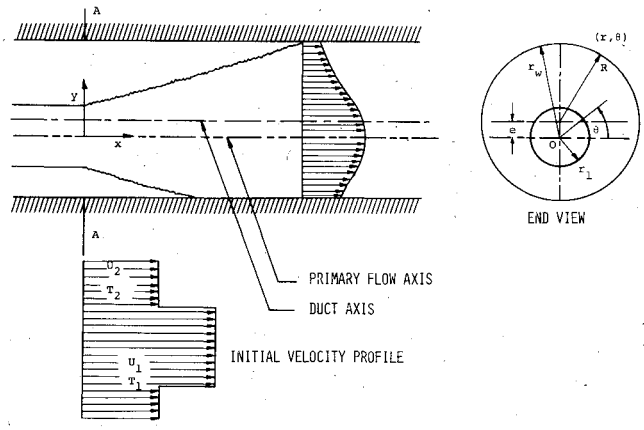

Fig. 2 Confined mixing with eccentricity.

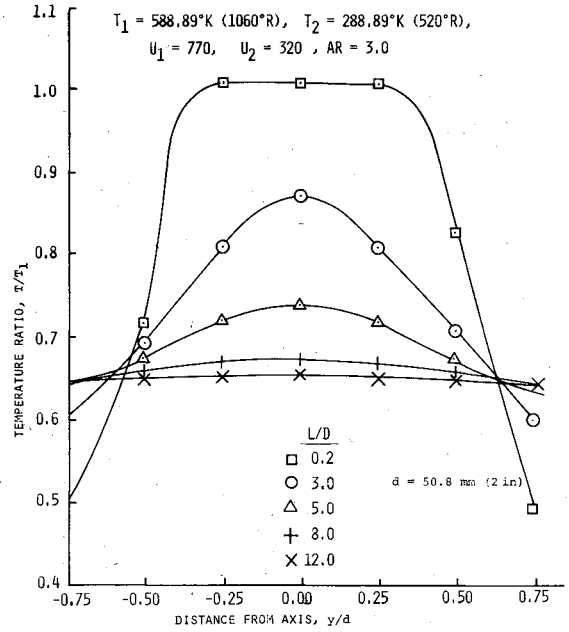

Fig. 3 Experimental temperature profiles for concentric case.

worked automatically for the complete run. Readings were taken at only five axial locations due to the run time limitation. The five locations corresponded to five cross sections located downstream of the initial mixing cross section at distances of 0.2, 3, 5, 8, and 12 times the internal diameter of the mixing duct. This procedure permitted fairly quick measurements with a temperature error of approximately ±2.778 K (±5°F) and a pressure error not greater than 5% for the case where the velocity was 60.96-121.92 m/s (200-400 ft/s).

The velocity was readily calculated from the formula

$$M^2 = \frac{2}{\gamma - 1}\left[\left(\frac{p_T}{p_s}\right)^{(\gamma-1)/\gamma} - 1\right] \tag{20}$$

since both the total and static pressure and temperature at a given point were known.

Experimental Results

Three different test configurations were employed during the total experiment. These were: 1) area ratio = 3.0 and $U_1 > U_2$; 2) area ratio = 3.0 and $U_1 < U_2$; 3) area ratio = 7.16 and $U_1 > U_2$.

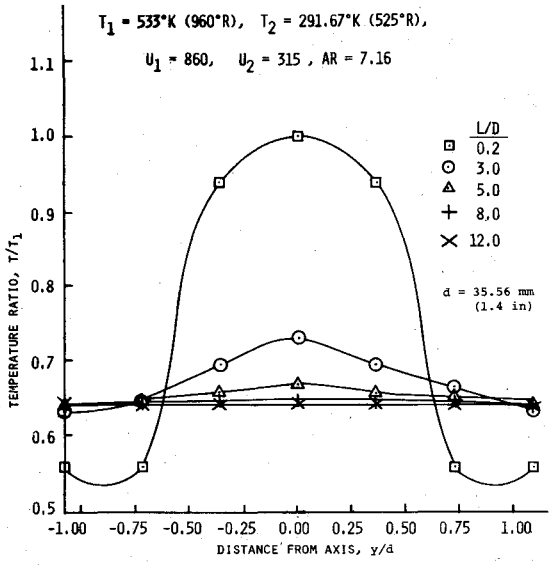

Fig. 4 Experimental temperature profiles for concentric case.

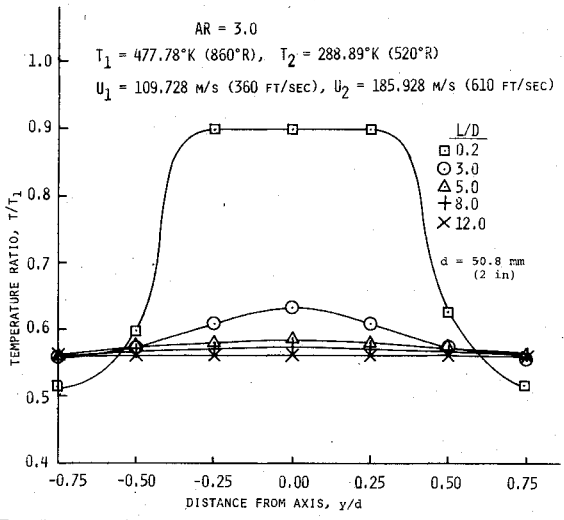

Fig. 5 Experimental temperature profiles for concentric case.

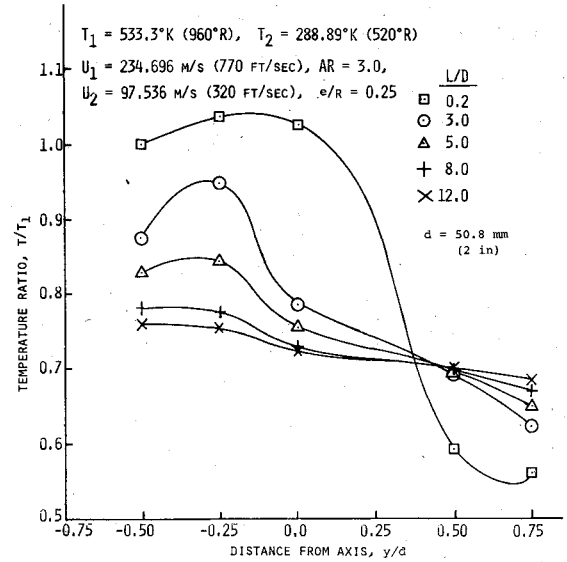

Fig. 6 Experimental temperature profiles for eccentric case.

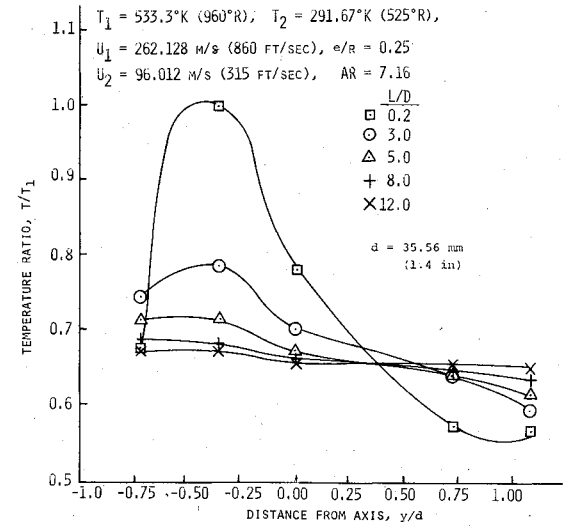

Fig. 7 Experimental temperature profiles for eccentric case.

Concentric Configuration

The experimental temperature profiles are plotted in Fig. 3 for the area ratio = 3.0, $U_1/U_2 = 2.4$, and $T_1/T_2 = 2.0$ at the five different cross sections. A fully developed temperature profile was obtained for most of the results at an L/D equal to 12. This means that the nonuniformity of the temperature profile has disappeared due to the high degree of mixing in the duct. From the data obtained, it was found that the larger the initial temperature ratio, the longer it takes for the flow to become completely mixed.

Figure 4 presents a plot of the experimental temperature profiles for the $U_1 > U_2$ case where the area ratio = 7.16. This area ratio was obtained by using a 35.56 mm (1.4 in.) diameter pipe inside the 101.6 mm (4.0 in.) diameter duct. Again the data taken at the five axial cross sections is plotted. A fully developed temperature profile is obtained at a distance equal to 12 times the diameter of the mixing duct ($L/D = 12.0$). The rate of decay of the temperature of the primary flow is higher than for the previous case where the area ratio was equal to three. In both cases $U_1 > U_2$.

Figure 5 is a plot of the experimental temperature profiles for the $U_1 < U_2$ case where the area ratio equals 3.0, the velocity ratio is 0.59, and the temperature ratio is 1.65. The final temperature is heavily influenced by the secondary stream temperature. This is due to the fact that the bypass ratio is high and the primary flow is rapidly damped out. From the many measurements which we have performed it was found in general that the low temperature ratios indicated more rapid mixing in the $U_1 > U_2$ and $U_1 < U_2$ cases.

Eccentric Configuration

The first case is again the $U_1 > U_2$ configuration at an area ratio equal to 3.0 and $e/R = 0.25$. Figure 6 represents the experimental temperature profiles at the five axial locations along the duct which were measured for this case. Figure 7 shows a configuration where $U_1 > U_2$, but the area ratio is equal to 7.16. The temperature and velocity ratio values are a repeat of the same values used for concentric mixing. Figure 8 represents the $U_1 < U_2$ configuration at an area ratio of 3.0. The same velocity ratios as the concentric experiments were used.

From the temperature curves presented in Figs. 6-8, it is apparent that the temperature profiles are always unsymmetrical about the axis of the mixing duct. At the cross sections near the initial cross section, the maximum temperature is at the axis of the primary flow. But as one proceeds downstream, the peak temperature tends to move toward the wall on the side of the eccentricity. Additionally, the temperature nonuniformity does not decay with the same rate as in the case of concentric mixing. The temperature decays more rapidly with increasing area ratio and when

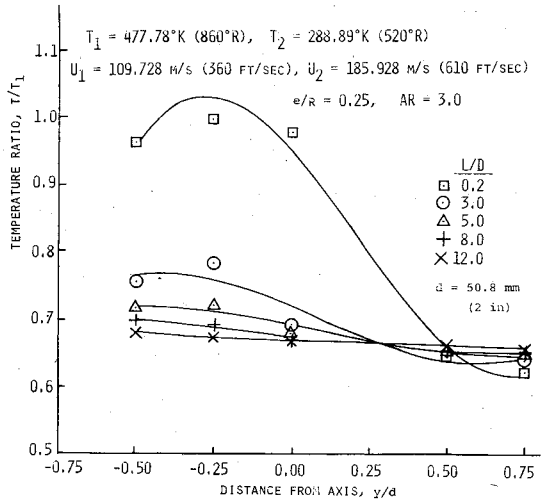

Fig. 8 Experimental temperature profiles for eccentric case.

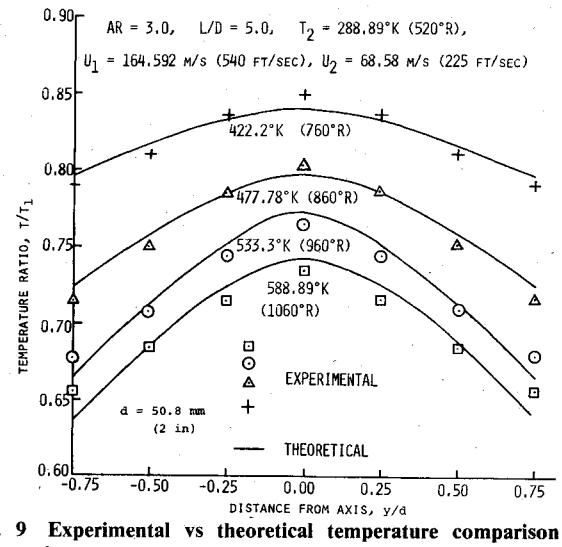

Fig. 9 Experimental vs theoretical temperature comparison for concentric case.

$U_1 < U_2$, which agrees with the expected result. All three configurations behave in the same general fashion with regard to temperature profile decay. The profile remains unsymmetrical even at the final cross section measured (i.e., $L/D = 12.0$). It is seen that eccentricity increases the axial distance required for a fully developed profile to be obtained. The rate of decay of the temperature profiles does not appear to have a direct relationship to either the primary temperature magnitude or the temperature ratio. The rate of decay appears to be fairly consistent with respect to these variables.

Results and Discussion

A preliminary examination of the test data indicated that the temperature mixing was much more rapid than the theory predicted. Therefore, based on the experience of Ref. 18, where a new value for the constant of turbulence C for the main region was experimentally obtained, a computer check was made on other values of C. It was found that increasing the value of C, even to a value of 20, did not significantly improve the agreement between the theoretical and experimental data. Another approach was deemed necessary. Following the background and reasoning of Ref. 18, the values of the temperature at the axis T_m and the temperature near the wall outside the boundary layer T_w were plotted for various values of L/D along the mixing duct. Instead of changing the values of C, however, the value of C_H, the constant of turbulence in the initial region, was varied and the resulting theoretical values of T_m and T_w were plotted. It was apparent that the initial temperature difference of the two streams caused the mixing to be accelerated. Therefore, it was reasonable to assume that the accelerated mixing would also affect the mixing in the initial region and hence shorten the axial length of the initial region. Various values of C_H were plotted against the experimental data and it was found that a value of $C_H = 0.36$ presented the best agreement between the theory and the experimental data. The physical explanation of the increase of the constant of turbulence is the effect of the confined wall.

With this value of $C_H = 0.36$ and the value of $C = 0.7$, the computer program was run to obtain the theoretical curves used to compare with the experimental data.

Theoretical vs Experimental Mixing Comparison for the Concentric Case

As was previously discussed, a new value of the constant of turbulence for the initial region was required to account for the increased degree of mixing which was exhibited by the experimental data. This new value helped in the agreement of the theoretical and experimental data for the cases where $U_1 > U_2$. It did not help in the $U_1 < U_2$ cases. Using the new value of the constant of turbulence ($C_H = 0.36$), a comparison between theory and experiment was made with plots for the following cases.

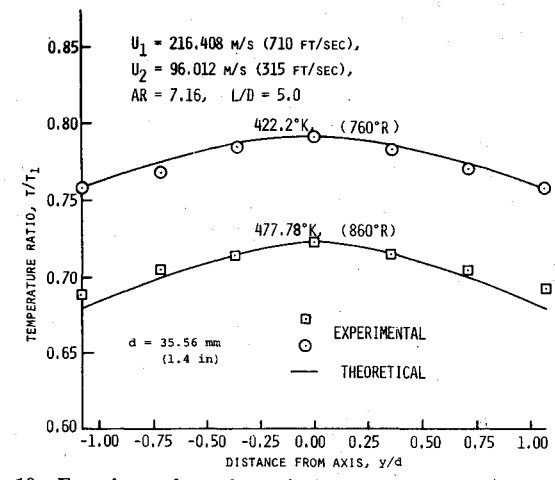

Fig. 10 Experimental vs theoretical temperature comparison for concentric case.

Case I: $U_1 > U_2$, $T_1 > T_2$, and $AR = 3.0$

Figure 9 illustrates this case for velocity ratio of 2.4 approximately. Each curve on the figure represents a temperature profile at the given cross section for different values of temperature ratio. The rapid degree of the disappearance of the initial temperature nonuniformity is readily apparent. The experimental temperature profile has a lower mean temperature than the theoretical temperature profile. This phenomenon was due to the heat loss through the wall of the duct. In general, the agreement between theory and experiment is fairly good.

Case II: $U_1 > U_2$, $T_1 > T_2$, and $AR = 7.16$

This case is illustrated by Fig. 10. Again a plot is made for a given velocity ratio and a given L/D with curves of two different temperature ratios. Because of the higher area ratio, the initial region length is decreased. The case II figure shows a lesser effect of heat loss. This is the expected result since the mass flow of cold secondary air compared to the mass flow of hot primary air is significantly larger than for case I. The lower average temperature in the partially mixed flow contributes to much less heat loss through the duct wall. The agreement between the case II experimental and theoretical temperature profiles is quite good.

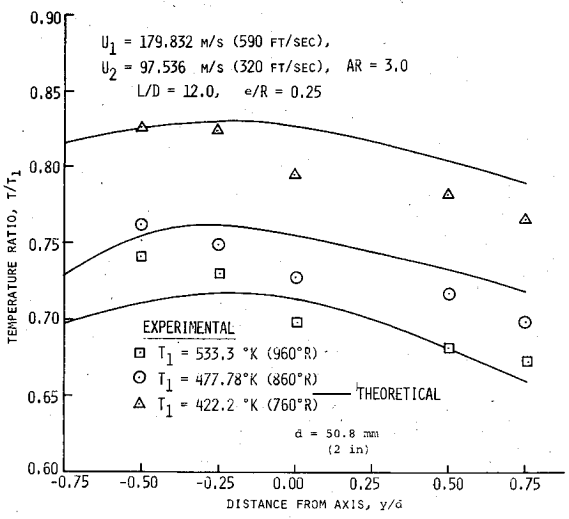

Fig. 11 Experimental vs theoretical temperature comparison for eccentric case.

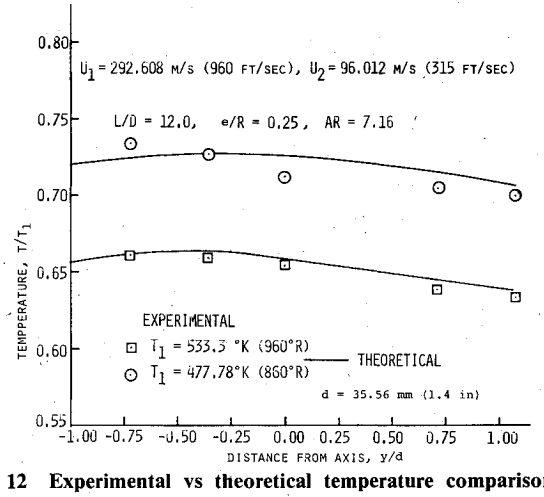

Fig. 12 Experimental vs theoretical temperature comparison for eccentric case.

Theoretical vs Experimental Mixing Comparison for the Eccentric Case

All the eccentric mixing cases were repeated for the concentric mixing cases with respect to the initial temperatures, velocities, and area ratios. The new value of the constant of turbulence in the initial region which was derived for the concentric mixing cases was used for the eccentric mixing cases. The same computer program could therefore be used for both mixing configurations. After examining the eccentric mixing comparisons of theoretical vs experimental temperature profiles, it was obvious that the good agreement exhibited by the concentric mixing data was no longer for the eccentric configurations. Two cases are presented.

Case I: $U_j > U_2$, $T_j > T_2$, $AR = 3.00$, $e/R = 0.25$, *and* $L/D = 12$

Figure 11 illustrates the case for velocities $U_j = 179.832$ m/s (590 ft/s), $U_2 = 97.536$ m/s (320 ft/s), and for the three different temperature ratios [$T_j = 533.3$, 477.78, and 422.2 K (960, 860, and 760°R); $T_2 = 288.89$ K (520°R)]. The agreement between theory and experiment is only fair for all cases plotted. It appears that the temperature ratio affects the degree of mixing inversely. This means that the lower temperature ratios produce better agreement with the theory.

Case II: $U_j > U_2$, $T_j > T_2$, $AR = 7.16$, $e/R = 0.25$, *and* $L/D = 12$

This case is illustrated in Fig. 12. Plot is made for velocities $U_j = 292.608$ m/s (960 ft/s) and $U_2 = 96.012$ m/s (315 ft/s) and for two different temperatures $T_j = 477.78$ and 422.2 K (960 and 860°R); the T_2 temperature was 294.4 K (530°R) for both cases. In general, the experimental data agrees better with the theory for this case compared to case I.

Conclusions

An experimental investigation of non-isoenergetic turbulent jet mixing between two streams in an axisymmetric duct has been conducted. Experimental temperature profiles have been measured at several axial locations in the duct. They have been compared with the theoretical temperature profiles determined by the analysis described in this paper. Several conclusions can be made from these comparisons.

It was determined that the theory and experimental results agree fairly well for the concentric case where the primary stream velocity is greater than the secondary stream velocity. This is true for both area ratios tested. The velocity ratio had no significant effect on the rate of temperature mixing of the flow. Also, contrary to the theory, the mixing process was not accelerated by a larger initial temperature difference between the flows. The opposite effect appeared to be the actual effect. It was experimentally verified, however, that energy diffuses more rapidly than momentum. The rate of mixing determined by the concentric mixing experiments indicated that the mixing was more rapid than the theoretical analysis had predicted. The eccentric experimental data did not agree with the theory as well as the concentric data. The 7.16 area ratio case produced better agreement than the 3.0 area ratio.

The theory used in this analysis is a fairly simple one which produces reasonably good results. Elimination of some of the simplifying assumptions should provide better agreement with the experimental data.

Acknowledgment

This work was sponsored by the U.S. Army Research Office—Durham, under Contract DAHC04-69-C-0016.

References

[1] Hartmann, A., "Theoretical and Experimental Investigation of Fan-Engines with Mixing: Optimal Layout of Fan-Engines with and without Mixing," AIAA Paper 67-416, July 1967.

[2] Khanna, K. K. and Tabakoff, W., "A Study of Non-Isoenergetic Turbulent Jet Mixing Between Compressible Subsonic Streams in Axisymmetric Constant Area Duct," University of Cincinnati, Ohio, Project Themis Rept. 69-1, Aug. 1969 (AD 696439).

[3] Abramovich, G. N., *The Theory of Turbulent Jets*, MIT Press, Cambridge, Mass., 1963.

[4] Alpinieri, L., "Turbulent Mixing of Coaxial Jets," *AIAA Journal*, Vol. 2, Sept. 1964, pp. 1560-1567.

[5] Maise, G. and McDonald, H., "Mixing Length and Kinematic Eddy Viscosity in a Compressible Boundary Layer," *AIAA Journal*, Vol. 6, Jan. 1968, pp. 73-80.

[6] Hinze, J., *Turbulence, An Introduction to Its Mechanism and Theory*, McGraw Hill Book Co., New York, 1959.

[7] Bradshaw, P., Ferriss, D., and Atwell, N., "Calculation of Boundary Layer Development Using the Turbulent Energy Equation," *Journal of Fluids Mechanics*, Vol. 28, Pt. 3, 1967, pp. 593-616.

[8] Zawacki, T. and Weinstein, H., "Experimental Investigation of Turbulence in the Mixing Region Between Coaxial Streams," NASA CR-959, Feb. 1968.

[9] Ortwerth, P., "Mechanism of Mixing of Two Non-Reacting Gases," AFAPL-TR-71-18, Oct. 1971.

[10] Edelman, R. and Fortune, O., "An Analysis of Mixing and Combustion in Ducted Flows," AIAA Paper 68-114, 1968.

[11] Hill, P., "Turbulent Jets in Ducted Streams," *Journal of Fluid Mechanics*, Vol. 22, Pt. 1, 1965, pp. 161-186.

[12] Drewry, J., "Supersonic Mixing and Combustion of Confined Coaxial Hydrogen-Air Streams," AIAA Paper 72-1178, Dec. 1972.

[13] Hendricks, C. and Brighton, J., "Prediction of Swirl and Inlet Turbulence Kinematic Energy Effects on Confined Jet Mixing," ASME Paper 75-FE-2, Jan. 1975.

[14] Hedges, K. and Hill, P., "Compressible Flow Ejectors, Part I," ASME Paper 74-FE-1, Feb. 1974.

[15] Hedges, K. and Hill, P., "Compressible Flow Ejectors, Part II," ASME Paper 74-FE-2, Feb. 1974.
[16] Burley, R. and Bryant, L., "Experimental Investigations of Coaxial Jet Mixing of Two Subsonic Streams at Various Temperature, Mach Number, and Diameter Ratios for Three Configurations," NASA Memo 12-21-58E, Feb. 1959.
[17] Razinsky, E., "Turbulent Mixing of Confined Axisymmetric Jets," University Microfilms, Ann Arbor, Mich., 1969.
[18] Tabakoff, W. and Hosny, W., "Theoretical and Experimental Investigations on the Mixing of Isoenergetic Confined Coaxial Jets," University of Cincinnati, Ohio, Project Themis Rept. 70-10, June 1970 (AD 710284).
[19] Tabakoff, W. and Hosny, W., "Theoretical and Experimental Jet Mixing of an Eccentric Primary Jet in a Constant Area Duct," University of Cincinnati, Ohio, Project Themis Rept. 70-11, July 1970 (AD 712333).
[20] Harsha, P. T., "Prediction of Free Turbulent Mixing Using a Turbulent Kinetic Energy Method," Langley Working Conference on Free Turbulent Shear Flows, NASA Langley Research Center, July 1972.
[21] Harsha, P. T., "Free Turbulent Mixing: A Critical Evaluation of Theory and Experiment," AEDC TR 71-36, Feb. 1971.
[22] Harsha, P. T. and Lee, S. C., "Analysis of Coaxial Free Mixing Using the Turbulent Kinetic Energy Method," *AIAA Journal*, Vol. 9, Oct. 1971, pp. 2063-2066.
[23] Lee, S. C. and Harsha, P. T., "Use of Turbulent Kinetic Energy in Free Mixing Studies," *AIAA Journal*, Vol. 8, June 1970, pp. 1026-1032.